

# UCSF

## UC San Francisco Previously Published Works

### Title

Tropism-modified AAV Vectors Overcome Barriers to Successful Cutaneous Therapy

### Permalink

<https://escholarship.org/uc/item/7w73n4q4>

### Journal

Molecular Therapy, 22(5)

### ISSN

1525-0016

### Authors

Sallach, Jessica  
Di Pasquale, Giovanni  
Larcher, Fernando  
et al.

### Publication Date

2014-05-01

### DOI

10.1038/mt.2014.14

Peer reviewed

# Tropism-modified AAV Vectors Overcome Barriers to Successful Cutaneous Therapy

Jessica Sallach<sup>1,2</sup>, Giovanni Di Pasquale<sup>3</sup>, Fernando Larcher<sup>4</sup>, Nadine Niehoff<sup>1,5</sup>, Matthias Rübsam<sup>1,5</sup>, Anke Huber<sup>1,2</sup>, Jay Chiorini<sup>3</sup>, David Almarza<sup>4,10</sup>, Sabine A Eming<sup>1,5,6</sup>, Hikmet Ulus<sup>7</sup>, Stephen Nishimura<sup>8</sup>, Ulrich T Hacker<sup>9</sup>, Michael Hallek<sup>1,2</sup>, Carien M Niessen<sup>1,5,6</sup> and Hildegard Büning<sup>1,2</sup>

<sup>1</sup>Center for Molecular Medicine Cologne (CMMC), University of Cologne, Cologne, Germany; <sup>2</sup>Department I for Internal Medicine, University Hospital Cologne, Cologne, Germany; <sup>3</sup>Molecular Physiology and Therapeutics Branch, National Institute of Dental and Craniofacial Research, National Institutes of Health, Bethesda, Maryland, USA; <sup>4</sup>Centro de Investigacion Energetica Medioambiental y Tecnologica (CIEMAT) Madrid, Center for Biomedical Research on Rare Diseases (CIBERER-U714) and Department of Bioengineering, Universidad Carlos III de Madrid (UC3M), Madrid, Spain; <sup>5</sup>Department of Dermatology, University Hospital of Cologne, Cologne, Germany; <sup>6</sup>Cologne Excellence Center on Cellular Stress Responses in Aging-Associated Diseases (CECAD), Cologne, Germany; <sup>7</sup>Children's Medical Surgery, Cologne, Germany; <sup>8</sup>Department of Pathology & Laboratory Medicine, Anatomic Pathology, UCSF, San Francisco, CA, USA; <sup>9</sup>University Cancer Center Leipzig (UCCL), Leipzig, Germany; <sup>10</sup>Current address: Molecular Immunology, UCL Institute of Child Health, London, UK.

Autologous human keratinocytes (HK) forming sheet grafts are approved as skin substitutes. Genetic engineering of HK represents a promising technique to improve engraftment and survival of transplants. Although efficacious in keratinocyte-directed gene transfer, retro-/lenti-viral vectors may raise safety concerns when applied in regenerative medicine. We therefore optimized adeno-associated viral (AAV) vectors of the serotype 2, characterized by an excellent safety profile, but lacking natural tropism for HK, through capsid engineering. Peptides, selected by AAV peptide display, engaged novel receptors that increased cell entry efficiency by up to 2,500-fold. The novel targeting vectors transduced HK with high efficiency and a remarkable specificity even in mixed cultures of HK and feeder cells. Moreover, differentiated keratinocytes in organotypic airlifted three-dimensional cultures were transduced following topical vector application. By exploiting comparative gene analysis we further succeeded in identifying  $\alpha v \beta 8$  integrin as a target receptor thus solving a major challenge of directed evolution approaches and describing a promising candidate receptor for cutaneous gene therapy.

Received 3 September 2013; accepted 11 January 2014; advance online publication 25 February 2014. doi:10.1038/mt.2014.14

## INTRODUCTION

The skin is a highly specialized barrier that protects the organism from environmental challenges while preventing loss of water and small nutrients.<sup>1,2</sup> The skin's most outer layer, the epidermis, is a stratified, multilayered epithelium consisting of the stratum basale, the stratum spinosum, the stratum granulosum and the stratum corneum.<sup>1,2</sup> To maintain proper protection against dehydration and the environment, the barrier is not static but requires continuous renewal. This is achieved by a tightly controlled balance between lifelong self-renewal of cells in the stratum basale

and a strictly regulated spatiotemporal terminal differentiation program, which ultimately leads to the formation of the stratum corneum, representing a water impermeable layer of avital cornified cells.<sup>3</sup>

Insults to the barrier including skin wounding initiate a well-coordinated process to restore skin barrier function that—depending on the insult—includes cell proliferation, migration, extracellular matrix deposition, angiogenesis, and skin remodeling.<sup>4</sup> This process fails in conditions of large cutaneous burns and chronic wounds. Limiting factors are the size of damage, an altered, inflammatory environment and/or lack of proper angiogenesis. Regenerative medicine has shown therapeutic promise in these settings. Specifically, autologous keratinocytes are grown on either artificial or natural supporting scaffolds and skin sheets are subsequently transplanted. Engraftment as well as wound closure can be significantly improved if the transplant secretes anti-inflammatory cytokines and/or growth factors including angiogenic mediators.<sup>5</sup> These factors are only transiently required arguing for the use of nonintegrating vectors for gene delivery.

Adeno-associated virus (AAV)-based vectors—classified as nonintegrating vectors—have emerged as one of the most promising delivery system for clinical use.<sup>6</sup> They are of low immunogenicity, can be produced at very high titers and deliver DNA vector genomes, which form episomes serving as templates for transcription.<sup>7</sup> The prototype AAV vector is based on the serotype 2 (AAV2). It can be pseudotyped with capsids of other natural occurring serotypes or with engineered capsids.<sup>7</sup>

AAV vectors have been successfully applied in over 80 clinical trials with an excellent safety profile.<sup>7</sup> Clinical benefit was reported for the treatment of a range of inherited diseases such as hemophilia B, Leber's congenital amaurosis or lipoprotein lipase deficiency.<sup>6</sup> The use of this vector system for the treatment of inherited skin diseases or in impaired wound healing, however, has been hindered by the refractoriness of primary human keratinocytes (HK) towards AAV-mediated transduction.<sup>8–12</sup>

The first two authors contributed equally to this work.

Correspondence: Hildegard Büning, Center for Molecular Medicine Cologne (CMMC), University of Cologne, Robert-Koch-Str. 21, 50931 Cologne, Germany. E-mail: [hildegard.buening@uk-koeln.de](mailto:hildegard.buening@uk-koeln.de)

Poor transduction activity can be addressed by directing vectors towards a novel receptor that is expressed on the target cell, mediates vector internalization and induces a cellular program leading to nuclear delivery of vector genomes and transgene expression.<sup>7</sup> To this end, vectors can be equipped with ligands that are either noncovalently linked or genetically incorporated into viral capsid or envelope proteins, a technology termed cell entry targeting or transductional targeting.

Also, the capsid of AAV2 tolerates genetic incorporation of peptide ligands.<sup>7</sup> It is a 60mer composed of three different viral proteins (VP1 (90 kDa), VP2 (72 kDa), and VP3 (60 kDa)), which share most of their amino acid sequence.<sup>13</sup> This common region ("common VP3 region") is frequently exploited for insertion of peptide ligands as it forms the capsid exterior.<sup>14</sup> Of particular interest is amino acid position 587 located at the tip of a peak at the capsid's threefold symmetry axis.<sup>15</sup> Its exposed position facilitates receptor binding of inserted peptides. Furthermore, insertions at this site disrupt the primary receptor-binding motif, a prerequisite for approaches aiming to redirect the viral tropism.<sup>16–18</sup>

Rational design-based approaches to modify the viral tropism are challenged by the limited knowledge on ligands capable of directing target cell transduction. We and others have therefore developed a high-throughput screening technique, the AAV peptide display, to select in a directed evolution approach and within the physiological context of the viral capsid for appropriate ligands.<sup>19–21</sup>

Here, we have exploited this technology to develop AAV targeting vectors with a striking tropism for primary HK. In contrast to natural occurring AAVs, these novel vectors efficiently transduce HK in monocultures, show a remarkable specificity for HK in feeder layer cocultures and can be applied topically on airlifted three-dimensional (3D) organotypic skin cultures for transduction of differentiated keratinocytes. The latter feature is not only important in basic research, but represents a central prerequisite for future clinical applications. Finally, we established comparative gene analysis as a tool to identify receptors targeted by vectors selected in high-throughput screens. We thereby solved a major problem impeding the application of tropism-modified vectors and identified a novel candidate receptor for modifying keratinocytes in regenerative medicine and gene therapy.

## RESULTS

### Primary HK lack primary receptor for AAV2

Previous studies have demonstrated that HK are poor targets for AAV2 vectors.<sup>8–12</sup> In line, transduction of HK, isolated from foreskins of different healthy donors, did not exceed 5% (Figure 1a). To unravel the cause for this refractoriness, keratinocytes were analyzed for the presence of receptors required for cell transduction by flow cytometry revealing that HK do express AAV2's internalization receptors  $\alpha v\beta 5$  and  $\alpha 5\beta 1$  integrin,<sup>22,23</sup> but lack heparan sulfate proteoglycan (HSPG), which serves as attachment receptor (Figure 1b).<sup>24</sup>

### High-throughput selection of AAV capsid variants on primary HK

To redirect the tropism of AAV vectors towards HK, we performed an AAV peptide display selection (Supplementary Figure S1) with a library that had been depleted for mutants displaying

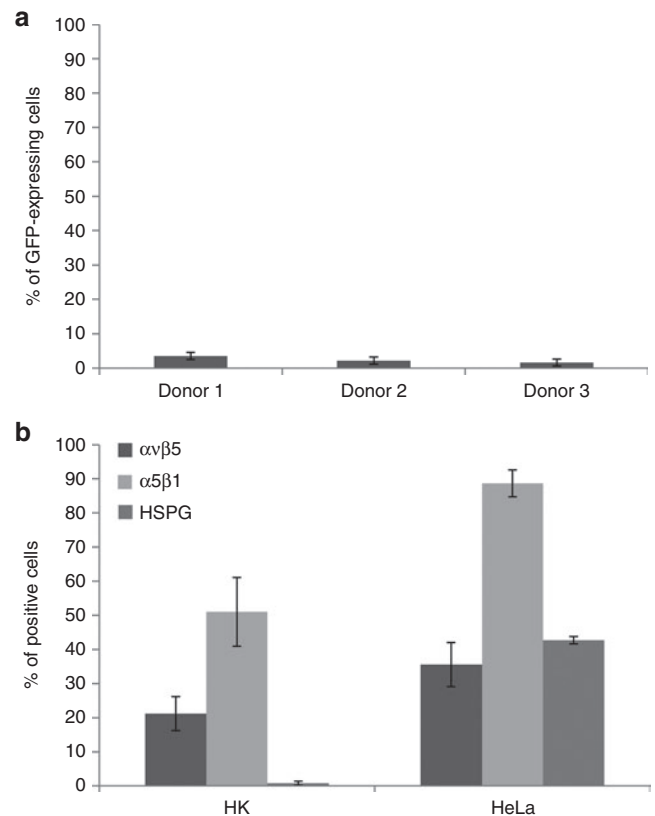


**Figure 1** Lack of receptor expression renders primary human keratinocytes (HK) refractory to transduction by AAV2. **(a)** Primary HK isolated from foreskins of three different healthy donors were incubated with  $5 \times 10^3$  vector genome containing particles (vg) per cell of AAV2. The AAV2 vector encoded for enhanced green fluorescent protein (GFP) in a self-complementary vector genome conformation. Percentage of transgene expressing cells was quantified by flow cytometry 48 hours posttransduction. Mean of three independent experiments  $\pm$  SD is shown. **(b)** HK and, as control, the cervix carcinoma cell line HeLa were stained with mouse antihuman  $\alpha v\beta 5$ , mouse antihuman  $\alpha 5\beta 1$  or mouse antihuman heparan sulfate proteoglycan (HSPG) antibody, followed by a phycoerythrin-labeled IgG secondary antibody. The percentage of cells positive for HSPG or integrin expression was quantified by flow cytometry. Mean of three independent experiments  $\pm$  SD is shown.

HSPG-binding peptides. Aiming to select for AAV variants that transduce HK with high efficiency and in a donor-independent manner, we used a different donor for each selection round and constantly increased the selection pressure by decreasing the number of particles from initially 1,000 vector genome containing particles (vg) per cell to 1 vg/cell.

After the 5th selection round, viral genomes were isolated and sequenced (Table 1). In total, nine different motifs were selected. With the exception of RSDLASL (Kera4) and PRGELAP (Kera5), all isolates encoded peptides with a RGD tripartite motif, a hallmark of integrin-binding ligands. Furthermore, in three of the nine motifs, the structure determining amino acid residue proline was located in position one and seven, and in three of the nine sequences the RGD motif was followed by leucine-alanine or leucine-arginine.

Three motifs with an overall neutral charge were picked for further analyses. Specifically, we choose Kera1 (RGDTATL) and Kera3 (RGDQQL), because of the high frequency of their occurrence, and Kera2 (PRGDLAP) because it contains the

leucine-alanine motif, the potential integrin-binding domain and flanking proline residues, which likely stabilizes presentation of the inserted peptide. The three capsid variants and AAV2 were packaged as vectors with a self-complementary vector genome encoding the enhanced green fluorescent protein (GFP) controlled by the cytomegalovirus promoter. The capsid-to-genomic particle

ratio for the AAV targeting vectors (AAV-Kera1, AAV-Kera2, and AAV-Kera3) and for AAV2 was comparable (**Supplementary Table S1**), indicating that none of the peptide insertions interfered with vector genome packaging.<sup>16</sup>

### AAV targeting vectors transduce primary HK with high efficiency in a peptide-dependent manner

To evaluate whether the targeting vectors indeed showed tropism for HK, we determined entry as well as transduction efficiency (**Figure 2**). For all three targeting vectors, a significantly increased number of intracellular vector genomes compared with AAV2 was measured. The most efficient vector, AAV-Kera2, demonstrated a 2,500-fold increase, followed by AAV-Kera3 (1,700-fold) and AAV-Kera1 (1,600-fold). Accordingly, also the transduction efficiency of the novel vectors was significantly higher compared with AAV2 (**Figure 2b**). Incubating HK for example with  $5 \times 10^3$  vg/cell resulted in transduction efficiencies of  $54.1\% \pm 11.6\%$  (AAV-Kera1),  $46.7\% \pm 16.8\%$  (AAV-Kera2), and  $47.0\% \pm 10.8\%$  (AAV-Kera3), while AAV2 failed to transduce HK ( $1.2\% \pm 0.5\%$ ) (**Supplementary Figure S2**).

Next, we performed competition assays with RGD- and RGE-containing peptides to prove that the RGD-containing peptide insertions were responsible for the improved transduction (**Figure 2c**).

**Table 1** Sequence and frequency of peptide insertions selected by AAV peptide display

Isolate	Sequence of insert	Frequency	Net charge
Kera1	RGDTATL	17	Neutral
Kera2	PRGDLAP	2	Neutral
Kera3	RGDQQSL	4	Neutral
Kera4	RSDLASL	3	Neutral
Kera5	PRGELAP	1	Neutral
Kera6	GRGDLAP	2	Neutral
Kera7	RGDTASL	1	Neutral
Kera8	PRGDLRP	4	Positive
Kera9	RGDQHSL	1	Positive

Sequence is shown as one letter code.

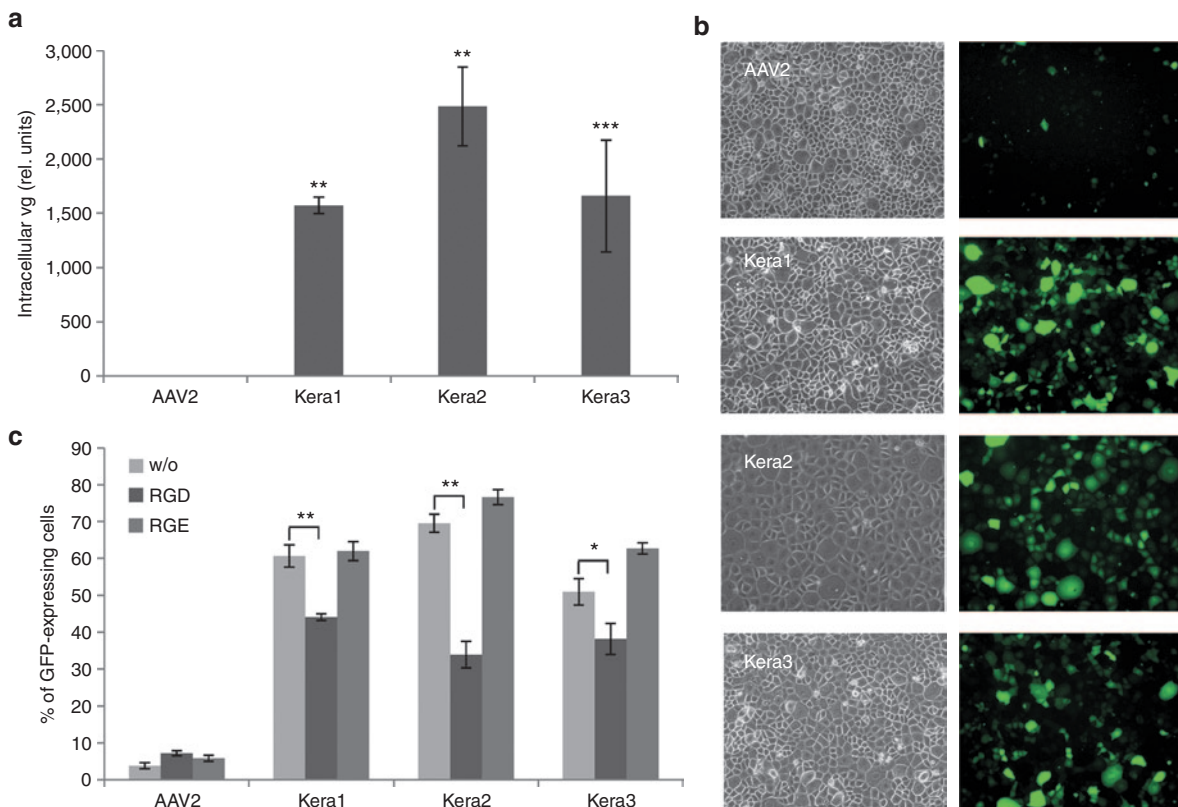


**Figure 2** Adeno-associated virus (AAV) targeting vectors show a peptide-mediated superior cell entry and transduction efficiency on human primary keratinocytes. Human keratinocytes (HK) seeded on collagen-precoated plates were incubated with the three AAV targeting vectors, AAV-Kera1 ("Kera1"), AAV-Kera2 ("Kera2"), and AAV-Kera3 ("Kera3"), and AAV2, respectively. **(a)** For measuring cell entry efficiency, cells were incubated with  $5 \times 10^2$  vg/cell. Cell transductions were stopped by extensive trypsin treatment to remove membrane-bound particles. Intracellular vector particles were quantified by qPCR and normalized to the housekeeping gene Plasminogen activator (PLAT). Values obtained for AAV2 were set to 1.  $n = 3$ ,  $**P < 0.01$ ,  $***P < 0.001$ . **(b)** HK seeded on collagen-precoated slides were incubated with indicated vectors ( $5 \times 10^4$  vg/cell) for 24 hours and analyzed microscopically. Original magnification: 40x. **(c)** HK were incubated with  $5 \times 10^3$  vg/cell of AAV2 or with  $7.5 \times 10^2$  vg/cell of the targeting vectors in the presence or absence of 300  $\mu\text{mol/l}$  GRGDS or GRGES peptides. The percentage of transgene (GFP) expressing cells was quantified by flow cytometry 48 hours posttransduction. Mean of three independent experiments  $\pm$  SD is shown.  $*P < 0.05$ ,  $**P < 0.01$ .

As control, we included AAV2 with an almost sevenfold higher vg/cell ratio than the targeting vectors. However, this was still not sufficient to achieve a transduction efficiency above background level (Figure 2c). In contrast, all three targeting vectors transduced HK with a vg/cell ratio of  $7.5 \times 10^2$  with efficiencies of  $51.0\% \pm 4.2\%$  (AAV-Kera3) or higher. Transduction of HK by the three targeting vectors was significantly reduced in the presence of RGD-containing peptides, while addition of RGE-containing peptides did not compete with vector-mediated cell transduction (Figure 2c). The most dramatic decrease in cell transduction by addition of the RGD-containing peptide was observed for AAV-Kera2.

### AAV targeting vectors demonstrate redirected tropism

Having demonstrated a tropism for HK, we were interested in studying the interaction with cell types representing potential off-targets in cutaneous gene therapy approaches. To this end, we compared transduction efficiencies of AAV2 and our targeting vectors on fibroblasts (using NIH3T3 fibroblasts), melanocytes (using BLM melanoma cells) and liver cells (using HepG2 hepatoma cells). Specifically, fibroblasts were used since this cell type is not only frequently found in the dermis but because fibroblasts are used as feeder cells for *ex vivo* keratinocyte cultures during tissue engineering. Melanocytes were exploited as further example of a specialized cell type of the epidermis and liver cells were chosen since AAV2 tend to accumulate in liver tissue, following both local as well as intravenous application.

All cell lines were transduced in a dose-dependent manner by AAV2 highlighting the broad tropism of AAV vectors with wild-type capsids (Figure 3). HepG2 cells showed the highest level with up to  $77.3\% \pm 3.1\%$  of transduced cells, followed by BLM cells. The lowest transduction efficiency was measured for NIH3T3 cells ( $24.3\% \pm 3.6\%$ ). In contrast, transduction efficiencies of AAV-Kera1, AAV-Kera2, and AAV-Kera3 remained at background level even at a vg/cell ratio of  $5 \times 10^3$ .

Since many standard HK cell cultures rely on the use of fibroblast feeder layers we aimed to evaluate whether our targeting vectors retain tropism for keratinocytes under the specific conditions of such cocultures. We therefore incubated cocultures of HK and NIH3T3 cells with AAV-Kera1, AAV-Kera2 and AAV-Kera3, respectively. As indicated in Figure 4, all three targeting vectors showed a remarkable preference for keratinocytes. The most striking results were obtained with AAV-Kera2, which transduced 83.8% of keratinocytes, while only 7.1% of the fibroblasts were positive for GFP.

### Transduction of differentiated keratinocytes in human organotypic skin cultures

Upon exposure to an air-liquid interface keratinocytes form a multilayered epidermis that mimics an *in vivo* stratified epidermis including a stratum corneum.<sup>25</sup> These 3D organotypic skin cultures serve as model system for functional testing in basic and applied research.<sup>25</sup> However, at present, keratinocytes have to be genetically manipulated prior to seeding due to inefficiency of *in situ* gene transfer thus limiting the use of such cultures. We therefore assessed whether our targeting vectors—when applied on the top layer of 16-day-old organotypic skin cultures—transduce keratinocytes following multilayer formation, *i.e.*,

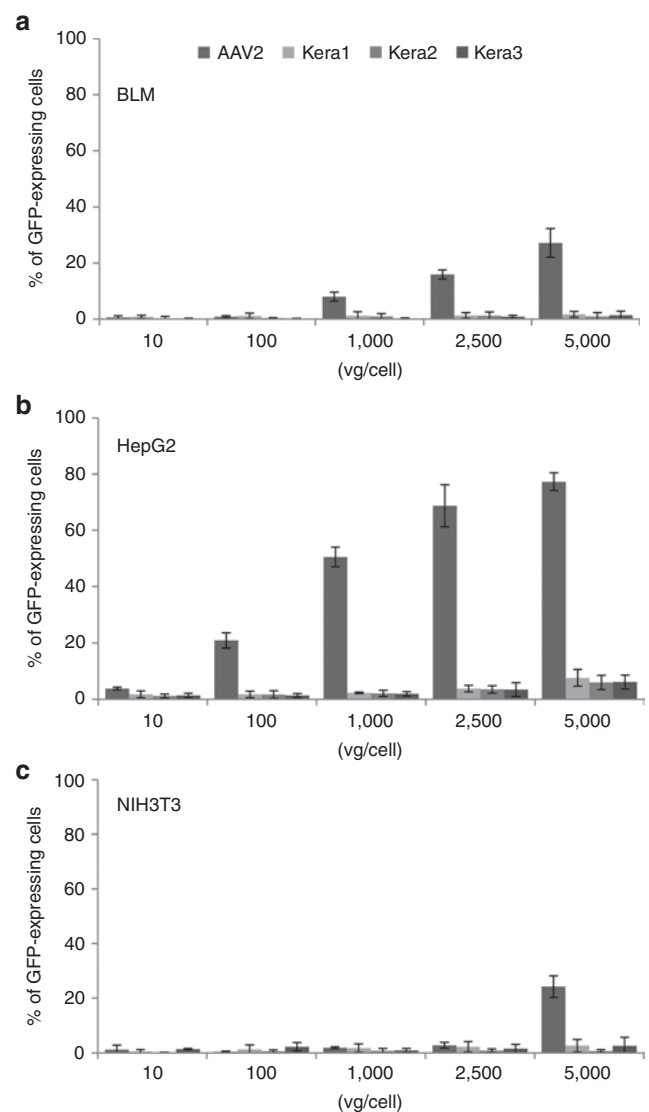


**Figure 3** Adeno-associated virus (AAV) targeting vectors show target cell selectivity. (a) The human melanoma cell line BLM, (b) the human hepatoma cell line HepG2, and (c) the mouse fibroblast cell line NIH3T3 were incubated with increasing vg/cell ratios of AAV-Kera1 ("Kera1"), AAV-Kera2 ("Kera2"), and AAV-Kera3 ("Kera3"), or AAV2, respectively. The percentage of transgene (GFP) expressing cells was quantified by flow cytometry 48 hours posttransduction. Mean of three independent experiments  $\pm$  SD is shown.

following differentiation. While no positive cells could be detected in phosphate-buffered saline (PBS)- or AAV2-treated cultures (Figure 5a), strong GFP signals were seen in the most upper layers of AAV-Kera2- and AAV-Kera3-treated 3D skin cultures with AAV-Kera2 also showing strong staining in lower keratinocyte layers (Figure 5b). Only weak GFP signals were detected in the AAV-Kera1-treated culture, suggesting that AAV-Kera1 was less efficient in transducing differentiated keratinocytes (Figure 5b).

### AAV targeting vectors transduce primary murine keratinocytes

Besides HK, primary murine keratinocytes (MK) are also used as targets for gene transfer but the efficiency of transfection is in

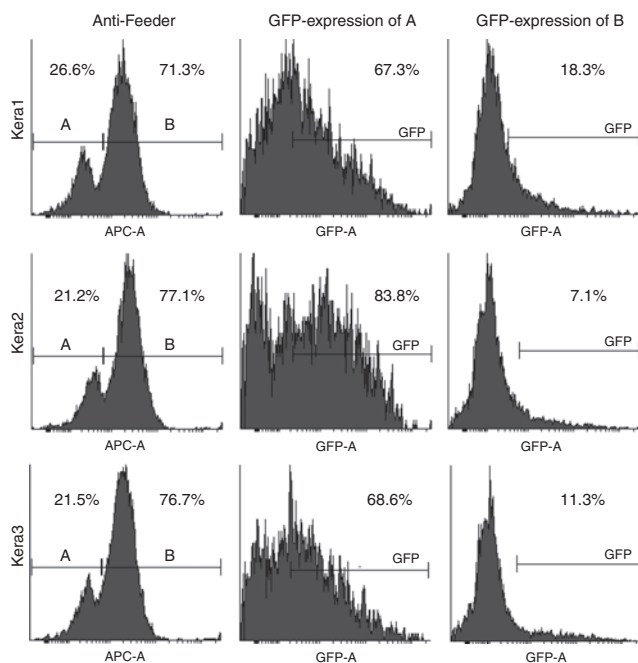


**Figure 4** Selective transduction of human primary keratinocytes in mixed cultures. Human keratinocytes (HK) were cocultured with NIH3T3 cells and incubated with the three targeting vectors for 48 hours. Cells were harvested and stained with an anti-Feeder antibody. Whole cell population stained with anti-Feeder antibody is indicated in the left column. Percentage of transduced cells in "A" and "B" was then determined. Percentage of GFP-expressing, but anti-Feeder negative cells (population "A," representing HK) is indicated in the middle, while percentage of GFP-expressing, anti-Feeder positive cells (population "B," representing fibroblasts) is shown in the right column. One representative experiment of three is shown.

general low. We therefore investigated whether our targeting vectors transduce primary MK. All three targeting vectors indeed transduced MK albeit with significant differences in efficiency (**Supplementary Figure S3a**). The highest transduction efficiency ( $30.9\% \pm 1.4\%$ ) was determined for AAV-Kera2, followed by AAV-Kera3 ( $20.2\% \pm 2.5\%$ ) and AAV-Kera1 ( $15.9\% \pm 2.3\%$ ). Of note, in contrast to HK, which are refractory to AAV2 transduction, incubation of MK with AAV2 lead to a transduction efficiency of  $12.3\% \pm 0.8\%$ . Thus, while AAV-Kera1 and AAV-Kera3 showed a similar efficiency than AAV2, AAV-Kera2 was significantly more efficient in transducing MK.

Next, we tested whether AAV-Kera2 is capable of transducing differentiated MK. We therefore applied AAV-Kera2 or PBS on the top layer of 15-day-old murine 3D organotypic skin cultures and determined transgene expression 72 hours later (**Supplementary Figure S3b**). While no positive cells could be detected in PBS-treated cultures, GFP signals were observed in the upper keratinocyte layer suggesting that also differentiated MK are targets for AAV-Kera2 transduction.

### Identification of candidate receptor by comparative gene analysis

So far, receptors used by AAV targeting vectors selected in high-throughput screens remained elusive, a drawback that may hamper their clinical use due to safety issues. Prompted by the success of comparative gene analysis (CGA), a microarray-based

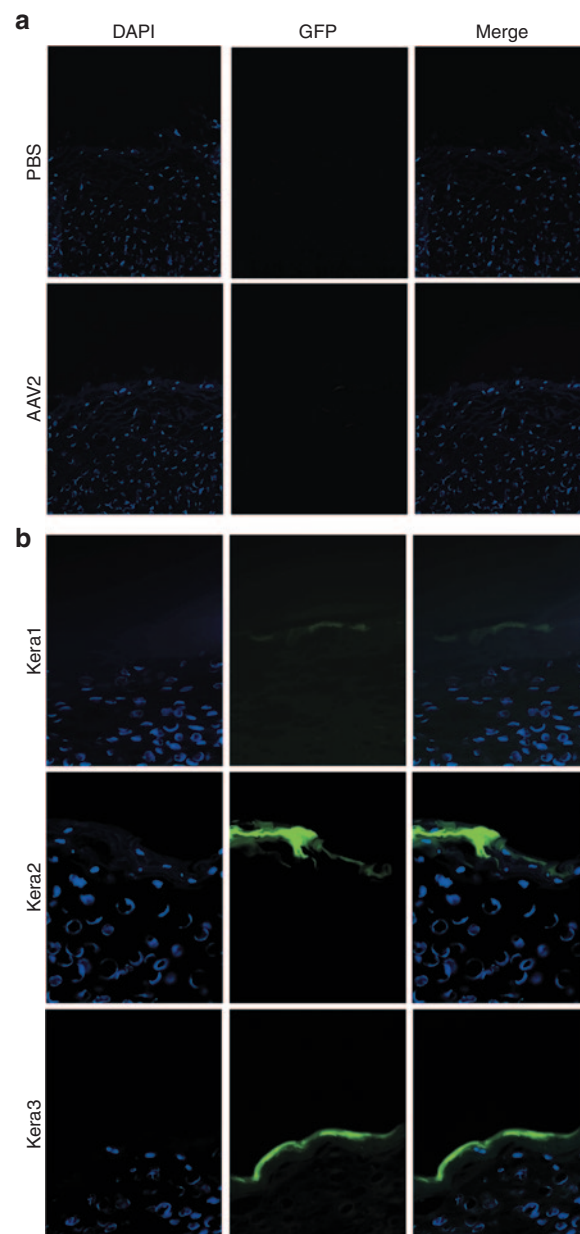


**Figure 5** Adeno-associated virus (AAV) targeting vectors transduce differentiated keratinocytes in organotypic cultures. Keratinocytes in organotypic three-dimensional skin cultures grow airlifted on the top of a collagen matrix containing fibroblasts. 16-day-old human three-dimensional skin cultures were incubated with (a) AAV2 or (b) AAV targeting vectors by dropping the vector solution into a glass ring placed on the top layer. (a) Control cultures received 1× phosphate-buffered saline (PBS). Vector solution was carefully and exhaustively removed after 2 hours, followed by culturing of the skin equivalents for further 72 hours. Samples were fixed and cryo-sections were mounted in IS Mounting Medium DAPI. Original magnification: (a), 20×; (b), 40×.

bioinformatic approach, in identifying receptors involved in transduction of natural occurring viruses,<sup>26–29</sup> we here aimed to exploit this method to map the receptor engaged by AAV-Kera2, the most efficacious of our three novel targeting vectors.

We therefore incubated 51 cell lines of the NCI60 cell line panel with AAV-Kera2 and, for comparison, with AAV2 followed by correlation of viral transduction with the cellular expression

profile of all genes in the COMPARE database. Genes associated with AAV-Kera2 transductions with a score equal or greater than 0.6 are shown as example in **Supplementary Table S2**.

The highest score for a cell membrane protein for AAV-Kera2 was obtained for *ITGB8* (a Pearson correlation coefficient of 0.72), the  $\beta 8$  integrin subunit. This gene positively correlated with multiple entries in the database (**Table 2**). In contrast, *ITGB8* appeared only once in the list of genes that correlated with AAV2 transductions (Pearson correlation coefficient value of 0.41).

### $\alpha v\beta 8$ integrin serves as receptor for AAV-Kera2

The  $\beta 8$  integrin subunit solely forms heterodimers with the  $\alpha v$  integrin subunit.<sup>30</sup> This integrin is expressed on HK (**Figure 6a**), but not on NIH3T3, BLM or HepG2 cells (**Figure 6b**), the cell lines for which AAV-Kera2 did not show tropism (**Figure 3**). As control for this, and as a defined model cell line for subsequent experiments, we included SW480 $\alpha v\beta 8$  (**Figure 6b**). This cell line stably expresses  $\alpha v\beta 8$  integrin as well as other  $\alpha v$ -containing integrins, while SW480, the parental cell line, expresses  $\alpha v$ , but not  $\alpha v\beta 8$  (**Supplementary Figure S4a**).<sup>31,32</sup> Both cell lines were transduced with equal efficacy by AAV2 (**Supplementary Figure S4b**). In contrast, we measured a significant higher transduction efficiency of AAV-Kera2 on SW480 $\alpha v\beta 8$  compared to SW480 cells (**Supplementary Figure S4b**), which is in concordance with involvement of  $\alpha v\beta 8$  integrin in AAV-Kera2-mediated transductions.

$\alpha v\beta 8$  integrin belongs to the group of integrins internalized through the clathrin pathway.<sup>33</sup> Thus, blocking this pathway by chlorpromazine that inhibits assembly of clathrin lattices,<sup>34</sup> should affect AAV-Kera2-mediated transduction of HK. As control, we performed cell transductions in the presence of genistein, which inhibits caveolin-mediated uptake.<sup>35</sup> In the presence of genistein, the transduction rate of AAV-Kera2 was improved (**Figure 6c**), maybe as result of an enhanced cellular uptake activity induced by inhibition of the caveolin pathway. In contrast, and in line with our hypothesis, addition of chlorpromazine, and thus inhibition of the clathrin pathway, significantly reduced the transduction efficiency of this vector (**Figure 6d**).

To provide further evidence for the involvement of  $\alpha v\beta 8$  integrin, we determined transduction efficiencies in the presence and absence of  $\alpha v$ - or  $\alpha v\beta 8$ -blocking antibodies. Neither the addition

of  $\alpha v$ - nor of  $\alpha v\beta 8$ -blocking antibodies negatively affected cell transductions by AAV2. Conversely, transductions by AAV-Kera2 were remarkably inhibited by 64.3% (anti- $\alpha v$ , **Figure 6e**) or 44.3% (anti- $\alpha v\beta 8$ , **Figure 6f**), respectively.

In support of these experimental data, sequence alignments revealed a striking homology between the AAV-Kera2 peptide sequence (PRGDLAP) and the binding motif (RGDLATI) of the high-affinity  $\alpha v\beta 8$  integrin ligand latency-associated peptide (LAP) of the transforming growth factor- $\beta$ .<sup>31,32</sup>

### DISCUSSION

Human skin equivalents are applied in conditions of impaired healing such as chronic wounds or large skin burns. While the pro-inflammatory microenvironment represents an important barrier for initial engraftment,<sup>36</sup> inadequate perfusion hampers long-term persistence of the skin equivalent.<sup>37</sup> Genetic modification of keratinocytes represents an attractive strategy to resolve these problems. Furthermore, cutaneous gene therapy may also be applied to a wide range of inherited skin blistering or barrier diseases for which no causal treatment is available yet.<sup>38</sup> To push cutaneous gene therapy towards clinical application, efficient and safe delivery tools are required. Here, we developed three highly efficient AAV targeting vectors (AAV-Kera1, AAV-Kera2 and AAV-Kera3) for genetic manipulation of human primary keratinocytes (HK), which transduce not only HK seeded as monolayers (**Figure 2**), but also showed tropism for keratinocytes in the presence of feeder cells (**Figure 4**). An important prerequisite for potential clinical use of vectors across the skin barrier is the ability to transduce differentiated keratinocytes. Applying our novel vectors to airlifted differentiated organotypic skin cultures revealed that in particular AAV-Kera2 is capable of transducing differentiated keratinocytes in 3D skin cultures (**Figure 5** and **Supplementary Figure S3b**). Our study is also the first that succeeded to identify a distinct receptor targeted by a capsid-modified vector selected in a directed evolution approach. Specifically, comparative gene analysis (CGA) revealed  $\alpha v\beta 8$  integrin as receptor engaged by AAV-Kera2, establishing thereby CGA as strategy to map receptors of capsid-modified vectors, and identified  $\alpha v\beta 8$  integrin as a promising novel candidate receptor for cutaneous gene therapy, which is of particular importance given the limited knowledge on receptors that can be exploited for modification of HK. These technical improvements open up the avenue for a plethora of new applications. More specifically, the novel vectors for example represent a promising tool for application in basic research and preclinical models, where they are expected to promote the analysis of protein function in keratinocyte monocultures and more importantly in skin equivalents by improving the efficiency of gene silencing, gene addition or gene correction approaches. This may lead to the development of novel treatment strategies including cutaneous gene therapy approaches. In this respect, AAV-Kera2's ability to transduce both primary human and murine keratinocytes (**Figure 2** and **Supplementary Figure S3**) is an important advantage. Moreover, in a clinical setting, the novel targeting vectors and here again in particular AAV-Kera2 represent efficient delivery tools for anti-inflammatory or pro-angiogenic genes to HK in order to improve engraftment and survival of skin transplants.<sup>36,37</sup> Since AAV-Kera2 possess the ability to transduce

**Table 2** The output of the COMPARE analysis

Gene	Symbol	Hits	Pearson correlation coefficient
Integrin, beta 8	ITGB8	11	0.72–0.5
Glypican 4	GPC4	3	0.67–0.65
Enabled homolog (Drosophila)	ENAH	3	0.63–0.53
Transmembrane and coiled-coil domain family 1	TMCC1	4	0.6–0.51
Prostaglandin-endoperoxide synthase 1	PTGS1	3	0.59–0.51
Kinesin family member 3A	KIF3A	2	0.56–0.52

Shown are the first six cell membrane genes that were associated with AAV-Kera2 transduction profile of the NCI60 cell panel. GeneCards symbols, number of hits, and the range of scores as Pearson correlation coefficient are also listed.

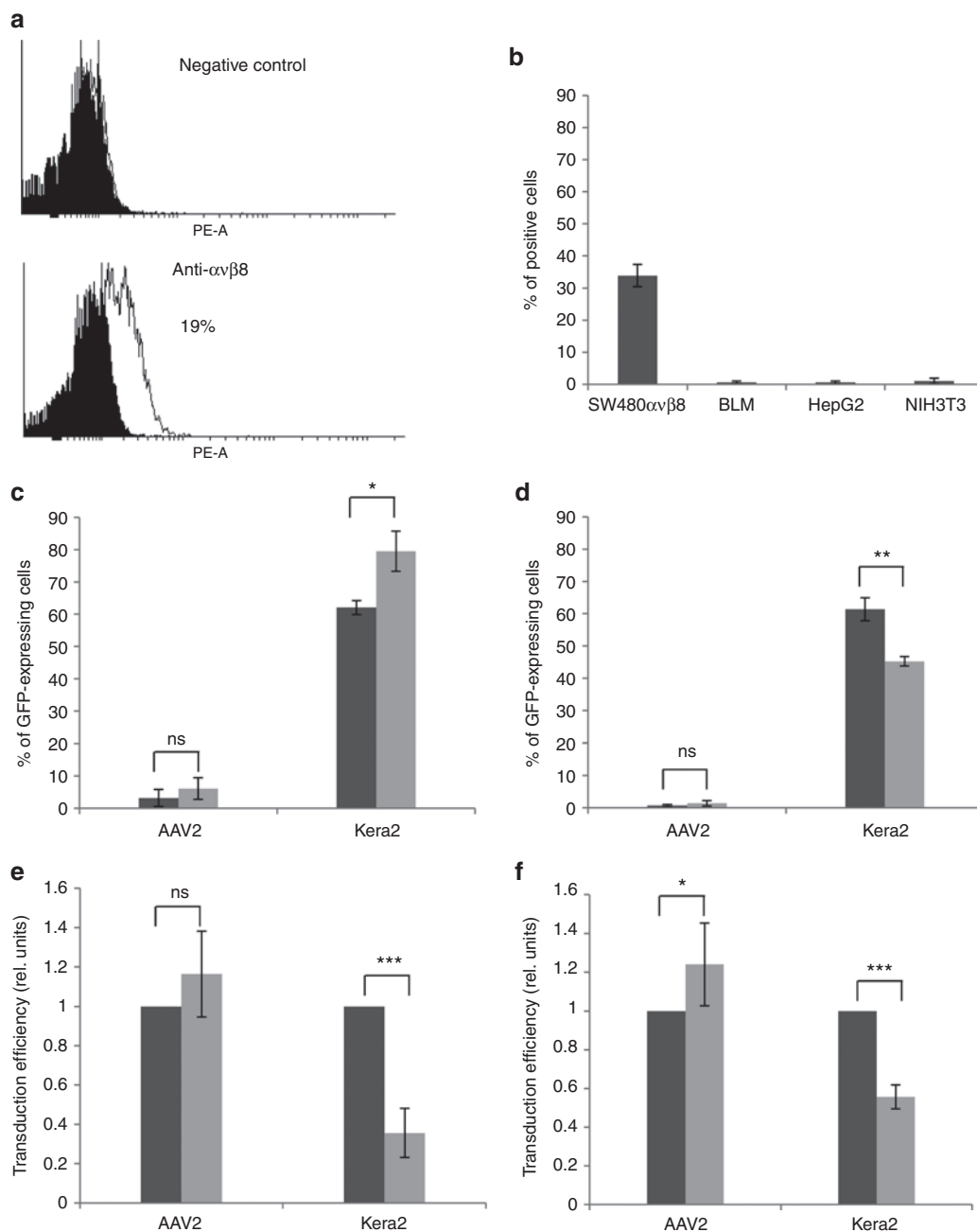


**Figure 6**  $\alpha v \beta 8$ -integrin serves as receptor for adeno-associated virus (AAV)-Kera2. **(a)** Human keratinocytes (HK) seeded on collagen precoated plates as well as **(b)** SW480 $\alpha v \beta 8$ , BLM, HepG2, and NIH3T3 cells were stained with antihuman  $\alpha v \beta 8$  antibody, followed by incubation with phycoerythrin (PE)-conjugated secondary antibody and flow cytometric measurements. **(c)** HK were incubated with  $5 \times 10^3$  vg/cell of AAV-Kera2 ("Kera2") or AAV2 in the absence (black) and presence (gray) of genistein (175  $\mu$ g/ml). **(d)** HK were incubated with  $3 \times 10^3$  vg/cell of AAV-Kera2 or  $5 \times 10^3$  vg/cell of AAV2 in the absence (black) and presence (gray) of chlorpromazine (16  $\mu$ g/ml). **(e)** SW480 $\alpha v \beta 8$  cells were incubated w/o (black) or with (gray) 2  $\mu$ g/ml of the  $\alpha v \beta 8$ -blocking antibody, followed by addition of  $6 \times 10^2$  vg/cell of AAV2 and AAV-Kera2, respectively. **(f)** SW480 $\alpha v \beta 8$  cells were incubated w/o (black) or with (gray) 200  $\mu$ g/ml  $\alpha v \beta 8$ -blocking antibody, followed by addition of  $7.5 \times 10^2$  vg/cell of AAV2 and  $3 \times 10^3$  vg/cell of AAV-Kera2, respectively. The percentage of GFP-expressing cells **(d-f)** was quantified by flow cytometry 48 hours posttransduction. In **a**, one representative experiment of three is shown. Values of **b-f** represent the mean of three independent experiments  $\pm$  SD. In **e** and **f**, values for nonantibody treated cells were set to 1. ns, nonsignificant, \* $p < 0.05$ , \*\* $p < 0.01$ , \*\*\* $p < 0.001$ .

also differentiated keratinocytes, the here-developed vectors are expected to also improve gene transfer efficiency following direct injection onto the wound bed. Finally, due to the knowledge on AAV-Kera2's receptor, local application of the vector to  $\alpha v \beta 8$  integrin-positive skin layers might possibly be used for *in vivo* gene transfer even in nonwounded skin.

Our novel vectors are based on AAV2, which do not show a natural tropism for keratinocytes (Figure 1a). Mechanistically, both cell entry and postentry barriers may hamper gene transfer efficiency. An example for the latter was previously reported by Braun-Falco and colleagues who improved keratinocyte transductions by addition of MG132, a proteasome inhibitor, or of



AG1478, an epidermal growth factor receptor protein tyrosine kinase (EGFR-PTK) inhibitor.<sup>8</sup> Both drugs impair degradation of incoming AAV2 particles by directly blocking proteasomal degradation (MG132) or by impairing EGFR-PTK-mediated phosphorylation of tyrosine residues of the AAV capsid, which promotes ubiquitination and thus degradation.<sup>39,40</sup>

Our study is indicative of the presence of an additional barrier, namely, the lack of HSPG (**Figure 1b**). This cell surface molecule is a component of the extracellular matrix and serves as attachment receptor for AAV2.<sup>24</sup> Site-directed mutagenesis of the HSPG binding motif<sup>6,17</sup> or presence of heparin, a soluble analogue of HSPG, during vector application renders AAV2 noninfectious<sup>24</sup> revealing the importance of HSPG for cell transduction. In order to explain this dependency, Asokan and colleagues postulated a conformational change of the capsid—induced by its binding to HSPG—that is required for binding to the internalization receptors.<sup>22</sup> So far, two different receptors for cell entry have been reported,  $\alpha 5\beta 1$  and  $\alpha v\beta 5$  integrin,<sup>22,23</sup> which—in contrast to HSPG—are both present on HK (**Figure 1b**).

The AAV peptide display technology represents a powerful tool to screen for viral variants that overcome both, pre- and postentry barriers, since this evolutionary approach selects for mutants capable of fulfilling the whole viral lifecycle, *i.e.*, generate progeny following target cell infection.<sup>19–21,41–44</sup> For selection of AAV variants targeting HK, we used our previous-described library of mutants displaying 7-mer random peptides at amino acid position 587.<sup>20</sup> Using this position for peptide insertion results in natural receptor-blinded mutants as the two main residues of the HSPG binding motif, R585 and R588, become separated.<sup>16–18</sup> Compared to previous AAV peptide display screens, we here implemented three technical improvements, which we believe are critical for selection of efficient targeting vectors with a redirected tropism: (i) the use of different donors in each selection round to avoid bias for receptors expressed in a donor-specific manner, (ii) continuous increase of the selection pressure by lowering the vg/cell ratio aiming to select for the fittest variants and (iii) the use of a library that had been depleted for AAV variants displaying HSPG binding peptides. Although HK lack HSPG expression, the latter step was included since mutants displaying such peptides like AAV2 tend to show a broad tropism<sup>45</sup> and to accumulate in liver and spleen,<sup>18</sup> which should be avoided in cutaneous gene therapy.

Sequencing of the viral progeny revealed selection of nine different peptide motifs (**Table 1**), three of which were chosen for further analyses based on the frequency of their occurrence (Kera1 and Kera3) or on the unique combination of prominent features (Kera2). All three targeting vectors (AAV-Kera1, -Kera2, and -Kera3) not only showed a donor-independent impressive increase in entry and transduction efficiency compared with AAV2 (**Figure 2** and **Supplementary Figure S2**), but also—in line with our hypothesis—a remarkable redirection of the tropism towards HK (**Figures 2–4**) arguing for the efficacy of our selection strategy.

Comparison with serotypes others than AAV2 further highlights the potency of the here-developed vectors. Ellis and colleagues compared nine different natural AAV serotypes (AAV1–AAV9) on 34 different cell lines and primary cell types

amongst them HK and MK.<sup>9</sup> The vectors, like ours, encoded for GFP controlled by the cytomegalovirus promoter in a self-complementary vector genome conformation. In contrast to our study, however, they performed all experiments with a vg/cell ratio of  $10^5$ . Of the nine serotypes, AAV6 was the most efficient vector transducing 80% of HK, followed by AAV1 (74%) and AAV3 (15%). Importantly, using a 20-fold lower vg/cell ratio, *i.e.*,  $5 \times 10^3$  vg/cell, we reached transduction efficiencies comparable to the most efficient serotype (AAV6), namely up to 83.8% (**Figure 4**). The same was true for MK, for which AAV1 is reported to be the most efficient serotype.<sup>9</sup> Again, using a 20-fold lower vg/cell ratio an equal transduction efficiency was reached (AAV1: 29% with a vg/cell ratio of  $10^5$  vs. AAV-Kera2:  $30.9\% \pm 1.4\%$  with a vg/cell ratio of  $5 \times 10^3$  (**Supplementary Figure S3a**)). Thus, with the here-developed vectors significantly lower particle numbers have to be applied to obtain transduction efficiencies similar to AAV1 and AAV6, the so far most efficient serotypes for primary keratinocytes.

Since each target cell type expresses a plethora of cell surface molecules, potentially serving as receptor, it is technically impossible to use high-throughput screens like the AAV peptide display for the selection of mutants specifically targeting a certain, beforehand chosen receptor. Due to the limited size of the selected peptide, it is also extremely unlikely to decipher the targeted receptor by a common data bank search. Thus, characterization of a specific receptor involved in retargeting represents an important so far unresolved challenge. To this end, we here exploited CGA as a novel strategy to identify the receptor targeted by the PRGDLAP peptide of AAV-Kera2, the targeting vector with the most striking tropism for HK. This screen revealed *ITGB8*, the integrin subunit  $\beta 8$ , as candidate.  $\beta 8$  is unique as it is solely described as heterodimer with  $\alpha v$ .<sup>30</sup> The only high-affinity ligand of  $\alpha v\beta 8$  integrin is the LAP of transforming growth factor- $\beta$ ,<sup>32</sup> which becomes thereby sequestered, a process crucial for maintaining epithelial homeostasis.<sup>32,46</sup> The binding of LAP to  $\alpha v\beta 8$  integrin is mediated by a RGDLATI motif located in the C'-terminal part of LAP, specifically at amino acid positions 244–250. Our selected peptide is a truncated version of this ligand as it contains the RGDLA motif flanked by two proline residues, which may stabilize this motif when displayed at the tip of the capsid peaks. Experimental evidence that  $\alpha v\beta 8$  serves as receptor for AAV-Kera2 is provided by the presence of this integrin on the target cells (**Figure 6**), the tropism of AAV-Kera2 for cells expressing  $\alpha v\beta 8$  integrin (compare **Figure 6a,b** with **Figures 2** and **3**; **Supplementary Figure S4**) and the significant inhibition of cell transduction in the presence of  $\alpha v$ - or  $\alpha v\beta 8$ -blocking antibodies (**Figure 6e,f**).

In summary, we here report on the development of three AAV2-based vectors for keratinocyte-directed gene transfer approaches that overcome the refractoriness of keratinocytes by targeting novel receptors. All three vectors showed tropism for keratinocytes in mono- and mixed cultures and for differentiated keratinocytes in organotypic 3D cultures, while transduction of off-target cell types remained at background level. Furthermore, we report on the first successful approach to identify candidate receptors engaged by tropism-modified AAV vectors, which as consequence revealed  $\alpha v\beta 8$  integrin as a promising candidate receptor for cutaneous gene therapy.

## MATERIALS AND METHODS

**Cell lines and primary cells.** The human embryonic kidney cell line HEK293 (ATCC number: CRL-1573), the human cervix carcinoma cell line HeLa (ATCC number: CCL-2), the human hepatoma cell line HepG2 (ATCC number: HB-8065), the human adenocarcinoma cell line SW480 and its derivative SW480 $\alpha$ v $\beta$ 8 (ref. 31) as well as the murine fibroblast cell line NIH3T3 (ATCC number: CRL-1658) were maintained in Dulbecco's modified Eagle's medium (DMEM) with GlutaMAX-I (Invitrogen, Karlsruhe, Germany). The human melanoma cell line BLM (kindly provided by Cornelia Mauch, University of Cologne, Germany) and the NCI60 cell line panel were maintained in RPMI-1640 medium with GlutaMAX-I (Invitrogen). All media were supplemented with 10% fetal calf serum (Invitrogen), 100 IU/ml of penicillin (Invitrogen) and 100  $\mu$ g/ml of streptomycin (Invitrogen). The medium of SW480 $\alpha$ v $\beta$ 8 and of the NCI60 cell line panel additionally contained 4  $\mu$ g/ml of puromycin (Invitrogen) and L-Glutamine 2 mmol/l (Invitrogen), respectively.

HK were isolated from human foreskin of healthy donors after informed consent (ethics committee vote: 12–163). Foreskin was separated manually into dermis and connective tissue. Dermis was minced into small pieces, transferred into Dispase II solution (10 mg/ml in DMEM/GlutaMAXTM-I (Invitrogen)) and incubated for 24 hours at 4 °C. Epidermis was detached from the dermis, followed by cell separation through trypsin/EDTA treatment. The suspension was filtered, pelleted by low speed centrifugation and cell pellet was resuspended in CnT Basal Medium 1 (CELLnTEC Advanced Cell Systems AG, Bern, Switzerland). Primary keratinocytes were isolated and cultured in minimal Ca<sup>2+</sup> medium (50  $\mu$ mol/l Ca<sup>2+</sup>) as described.<sup>47</sup>

**Antibodies and evaluation of cell surface expression of integrins and HSPG.** For determining cell surface expression of integrins and HSPG, respectively, the following antibodies were used: mouse antihuman  $\alpha$ v $\beta$ 5 antibody (MAB1961, Millipore, Schwalbach, Germany), mouse antihuman  $\alpha$ 5 $\beta$ 1 antibody (MAB1999, Millipore), mouse antihuman  $\alpha$ v antibody (MAB1953, Millipore), mouse antihuman  $\alpha$ v $\beta$ 8 antibody (37E5),<sup>31</sup> and mouse antihuman heparan sulfate delta (USBiological, Salem, MA). Cells were harvested by mechanically scraping, pelleted and resuspended in 1 $\times$  PBS. Indicated primary antibody was added and cells were incubated 15 minutes on ice followed by a washing step. Secondary antibody (goat antimouse IgG, Southern Biotech, Eching, Germany) was added to cell suspension in 1 $\times$  PBS. Following incubation on ice for 15 minutes and a further washing step, cells were analyzed by flow cytometry. A minimum of 10,000 cells was counted for each sample. Unstained cells and cells that were only treated with secondary antibody were used as controls.

**Selection of AAV capsid mutants on primary HK.** AAV peptide display selection on HK was performed using a library of AAV capsid insertion mutants depleted for mutants capable of binding to HSPG by heparin affinity chromatography.<sup>18</sup> Selection pressure was increased from round 1 to 5 by reducing the vg/cell number from 1,000 to 1. Following the 5th selection round, viral progeny was isolated and sequenced (Qiagen, Hilden, Germany).<sup>20</sup> The AAV helper plasmids pRC-Kera1, pRC-Kera2 and pRC-Kera3 were obtained by subcloning the BsiwI/SnaBI fragment of the AAV genome containing the respective insert sequences (Table 1) into pRC-K<sup>17</sup> from which the corresponding region had been removed.

**Production of recombinant AAV vectors.** HEK293 cells were seeded at 80% confluency and cotransfected with a total of 37.5  $\mu$ g of pRC,<sup>48</sup> pscAAV/EGFP,<sup>49</sup> and pXX6<sup>50</sup> for AAV2 production. For production of targeting vectors, pRC was exchanged for pRC-Kera1, pRC-Kera2, and pRC-Kera3, respectively. Forty-eight hours posttransfection, cells were harvested, lysed and purified by iodixanol density step gradient centrifugation.<sup>49</sup> Genomic particle titers were determined by qPCR (LightCycler System, Roche Diagnostics, Mannheim, Germany) using transgene specific primers.<sup>45</sup> The capsid titer was determined by enzyme-linked immunosorbent assay using the AAV2 capsid-specific antibody A20 (Progen, Heidelberg, Germany).

**Quantification of entry and transduction efficiency.** For determining entry efficiency HK, seeded at 70–80% confluency in collagen precoated wells, were incubated with the indicated vg/cell ratio for 30 minutes on ice and then shifted to 37 °C and 5% CO<sub>2</sub>. Cells were harvested 1 hour posttransduction (p.t.). The cells were washed and membrane-bound vector particles were removed by trypsin treatment.<sup>45</sup> Cell pellet was washed twice with 1 $\times$  PBS and total viral DNA was isolated (DNeasy Tissue Kit, Qiagen). Relative quantification of vector genomes (GFP) and reference gene (PLAT) was performed by qPCR (Roche Diagnostics).<sup>45</sup> The specificity of target and reference gene amplification was confirmed by melting-curve analysis. GFP values were normalized to PLAT levels using the LightCycler 480 software 1.5 (Roche Diagnostics).

For determining transduction efficiency, HK or indicated cell lines were incubated with the indicated vg/cell ratio for 48 hours, while MK were incubated with 5 $\times$ 10<sup>3</sup> vg/cell for 72 hours, followed by flow cytometry measurements (BD FACS Calibur). A minimum of 10,000 cells was counted for each sample. Background fluorescence was set to 1%. For mixed cultures, HK and NIH3T3 fibroblasts were seeded at a ratio of 1:1. Briefly, NIH3T3 cells were seeded in a collagen precoated 24-well plate and cultivated for 5 hours. Medium was carefully aspirated and HK were added. The number of HK were determined 24 hours later and mixed cultures were incubated with 5 $\times$ 10<sup>3</sup> vg/HK for 48 hours at 37 °C. Cells were harvested, stained with anti-Feeder antibody (monoclonal, APC conjugated mouse antihuman, Miltenyi, Bergisch Gladbach, Germany) and GFP-positive as well as APC-positive cells were determined by flow cytometry as described above.

**Competition and inhibition experiments.** HK, seeded in collagen precoated wells, were incubated with chlorpromazine at a final concentration of 16  $\mu$ g/ml or with genistein at a final concentration of 648  $\mu$ mol/l for 30 minutes at 37 °C or left untreated. Vectors were added at the indicated vg/cell ratio to drug-treated or -untreated cells. Drug treatment was stopped at indicated time points p.t. by washing, followed by extensive treatment with trypsin and reseeding of cells in fresh medium again on precoated plates. For peptide competition experiments, HK were incubated with 300  $\mu$ mol/l GRGDS or GRGES peptides or left untreated for 15 minutes at 37 °C. Subsequently, vectors were added at the indicated vg/cell ratio. At 4 hours p.t. cells were harvested and reseeded as described before. For the antibody blocking experiments cells were either incubated with 2  $\mu$ g/ml  $\alpha$ v-blocking antibody (Millipore) for 15 minutes at 37 °C or with 200  $\mu$ g/ml of  $\alpha$ v $\beta$ 8-blocking antibody<sup>31</sup> for 30 minutes on ice, followed by vector incubation. Cells incubated with vectors in the absence of antibodies served as control. Vectors were removed after 4 hours ( $\alpha$ v) or 30 minutes ( $\alpha$ v $\beta$ 8). Transduction efficacy was determined 48 hours p.t. by flow cytometry.

**Correlation of AAV-Kera2 transduction with NCI60 cell panel microarray gene expression pattern.** Fifty-one cell lines of the NCI60 panel were transduced with serially diluted AAV2 or AAV-Kera2 vectors. 48 hours p.t. cells were harvested and analyzed by flow cytometry to quantify GFP-positive cells using a BD FACSArray. The relative transduction efficiencies of the 51 cell lines were expressed as a pattern which we then used as a seed file for comparison to the patterns in the Developmental Therapeutics Program (DTP), National Cancer Institute (NCI) database, using the COMPARE algorithm ([http://dtp.nci.nih.gov/compare-web-public\\_compare/login.do](http://dtp.nci.nih.gov/compare-web-public_compare/login.do)). This algorithm determines the similarity of patterns between the given “seed” and others within a database by creating a scalar index of similarity expressed quantitatively as a pearson correlation coefficient. The output of the COMPARE program is a rank-ordered list (by pearson correlation coefficient) of the most highly correlated patterns from the database.

**Transduction of organotypic human 3D skin cultures.** A dermal equivalent consisting of a collagen gel populated with NIH3T3 fibroblasts was cultivated in DMEM/GlutaMAXTM-I medium supplemented with 10% fetal calf serum (Invitrogen), 100 U/ml penicillin (Invitrogen), 100  $\mu$ g/

ml streptomycin (Invitrogen), 10 µg/ml Transforming Growth Factor- $\alpha$  (Sigma-Aldrich, Taufkirchen, Germany), 10 µg/ml EGF (Sigma-Aldrich) and 50 µg/ml sodium L-ascorbate (Sigma-Aldrich). In case of the organotypic murine 3D skin culture, the collagen gel populated with NIH3T3 fibroblasts was cultivated in DMEM/Ham's F12 medium (Sigma-Aldrich) supplemented with 10% fetal calf serum Gold (PAA, Coelbe, Germany), 100 U/ml penicillin (Invitrogen), 100 µg/ml streptomycin (Invitrogen), 2 mmol/l L-Glutamine (Life Technologies GmbH, Darmstadt, Germany), 10 µg/ml EGF (Sigma-Aldrich), 50 µg/ml sodium L-ascorbate (Sigma-Aldrich), 5 µg/ml Insulin (Sigma-Aldrich), 0.5 µg/ml Hydrocortisone (Sigma-Aldrich),  $1 \times 10^{-10}$  mol/l cholera toxin (Sigma-Aldrich), and 0.2 mmol/l CaCl<sub>2</sub>. Keratinocytes were seeded in glass rings on top of the collagen gel submerged in medium for 24 hours at 37 °C. Glass rings were removed, medium was changed every other day with the liquid level just sufficient to contact the collagen gel, leaving the keratinocyte layer exposed to air. To transduce HK or MK, a sterile glass ring was put on top of the keratinocyte layer and filled with medium containing the indicated vector solution or 1× PBS. Two hours p.t., vector containing solution or 1× PBS was carefully removed. Organotypic cultures were cultivated for further 72 hours at 37 °C and subsequently fixed in 2% paraformaldehyde in 3.5% sucrose/1× PBS for 30 minutes at room temperature and embedded in Tissue Tek (Sakura Finetek, Zoeterwoude, Netherland). Cryo-sections (5 µm) were mounted by IS Mounting Medium DAPI (Dianova, Hamburg, Germany) and analyzed microscopically.

## SUPPLEMENTARY MATERIAL

**Figure S1.** Schematic overview of AAV peptide display selection.

**Figure S2.** Transduction efficiency of targeting vectors on primary human keratinocytes.

**Figure S3.** Transduction efficiency of targeting vectors on primary murine keratinocytes.

**Figure S4.** Presence of  $\alpha\beta 8$  integrins improves cell transduction.

**Table S1.** Packaging efficiency of AAV targeting vectors.

**Table S2.** Genes associated with AAV-Kera2 transduction.

## ACKNOWLEDGMENTS

This work was supported by grants from the Research Priority Program 1230 (SPP1230) "Mechanisms of gene vector entry and persistence" of the Deutsche Forschungsgemeinschaft (DFG) to H.B. (BU1310/1–2) and from the Center for Molecular Medicine Cologne (CMMC) to H.B. (B1). F.L. was supported by grants from Instituto de Salud Carlos III (PI11/01225) and Comunidad de Madrid (S2010/BMD-2359), S.A.E. by the CMMC (C1.1), S.N. by the National Institutes of Health (HL113032, NS044155) and M.H. by the European Union (LSHBCT-2005–512102). We thank Jude Samulski (University of North Carolina at Chapel Hill, NC) for providing plasmid pXX6, Vyomesh Patel (Oral & Pharyngeal Cancer Branch, National Institute of Dental and Craniofacial Research, National Institutes of Health, Bethesda, MD) for sharing reagents, and Hanna Janicki (University of Cologne, Germany), and Stephanie Cambier (UCSF, San Francisco, CA) for technical assistance. The authors declare no conflict of interest.

## REFERENCES

- Kubo, A, Nagao, K and Amagai, M (2012). Epidermal barrier dysfunction and cutaneous sensitization in atopic diseases. *J Clin Invest* **122**: 440–447.
- Simpson, CL, Patel, DM and Green, KJ (2011). Deconstructing the skin: cytoarchitectural determinants of epidermal morphogenesis. *Nat Rev Mol Cell Biol* **12**: 565–580.
- Fuchs, E (2007). Scratching the surface of skin development. *Nature* **445**: 834–842.
- Gurtner, GC, Werner, S, Barrandon, Y and Longaker, MT (2008). Wound repair and regeneration. *Nature* **453**: 314–321.
- Priya, SG, Jungvid, H and Kumar, A (2008). Skin tissue engineering for tissue repair and regeneration. *Tissue Eng Part B Rev* **14**: 105–118.
- Mingozzi, F and High, KA (2011). Therapeutic *in vivo* gene transfer for genetic disease using AAV: progress and challenges. *Nat Rev Genet* **12**: 341–355.
- Büning, H, Perabo, L, Coutelle, O, Quadt-Humme, S and Hallek, M (2008). Recent developments in adeno-associated virus vector technology. *J Gene Med* **10**: 717–733.
- Braun-Falco, M, Eisenried, A, Büning, H and Ring, J (2005). Recombinant adeno-associated virus type 2-mediated gene transfer into human keratinocytes is influenced by both the ubiquitin/proteasome pathway and epidermal growth factor receptor tyrosine kinase. *Arch Dermatol Res* **296**: 528–535.
- Ellis, BL, Hirsch, ML, Barker, JC, Connelly, JP, Steininger, RJ 3rd and Porteus, MH (2013). A survey of ex vivo/in vitro transduction efficiency of mammalian primary cells and cell lines with Nine natural adeno-associated virus (AAV1–9) and one engineered adeno-associated virus serotype. *Viral J* **10**: 74.
- Gagnoux-Palacios, L, Hervouet, C, Spirito, F, Roques, S, Mezzina, M, Danos, O *et al.* (2005). Assessment of optimal transduction of primary human skin keratinocytes by viral vectors. *J Gene Med* **7**: 1178–1186.
- Keswani, SG, Balaji, S, Le, L, Leung, A, Lim, FY, Habli, M *et al.* (2012). Pseudotyped adeno-associated viral vector tropism and transduction efficiencies in murine wound healing. *Wound Repair Regen* **20**: 592–600.
- Petek, LM, Fleckman, P and Miller, DG (2010). Efficient KRT14 targeting and functional characterization of transplanted human keratinocytes for the treatment of epidermolysis bullosa simplex. *Mol Ther* **18**: 1624–1632.
- Kronenberg, S, Kleinschmidt, JA and Böttcher, B (2001). Electron cryo-microscopy and image reconstruction of adeno-associated virus type 2 empty capsids. *EMBO Rep* **2**: 997–1002.
- Büning, H, Bolyard, CM, Hallek, M and Bartlett, JS (2011). Modification and labeling of AAV vector particles. *Methods Mol Biol* **807**: 273–300.
- Xie, Q, Bu, W, Bhatia, S, Hare, J, Somasundaram, T, Azzi, A *et al.* (2002). The atomic structure of adeno-associated virus (AAV-2), a vector for human gene therapy. *Proc Natl Acad Sci USA* **99**: 10405–10410.
- Kern, A, Schmidt, K, Leder, C, Müller, OJ, Wobus, CE, Bettinger, K *et al.* (2003). Identification of a heparin-binding motif on adeno-associated virus type 2 capsids. *J Virol* **77**: 11072–11081.
- Opie, SR, Warrington, KH Jr, Agbandje-McKenna, M, Zolotukhin, S and Muzyczka, N (2003). Identification of amino acid residues in the capsid proteins of adeno-associated virus type 2 that contribute to heparan sulfate proteoglycan binding. *J Virol* **77**: 6995–7006.
- Perabo, L, Goldnau, D, White, K, Endell, J, Boucas, J, Humme, S *et al.* (2006). Heparan sulfate proteoglycan binding properties of adeno-associated virus retargeting mutants and consequences for their *in vivo* tropism. *J Virol* **80**: 7265–7269.
- Müller, OJ, Kaul, F, Weitzman, MD, Pasqualini, R, Arap, W, Kleinschmidt, JA *et al.* (2003). Random peptide libraries displayed on adeno-associated virus to select for targeted gene therapy vectors. *Nat Biotechnol* **21**: 1040–1046.
- Perabo, L, Büning, H, Kofler, DM, Ried, MU, Girod, A, Wendtner, CM *et al.* (2003). *In vitro* selection of viral vectors with modified tropism: the adeno-associated virus display. *Mol Ther* **8**: 151–157.
- Varadi, K, Michelfelder, S, Korff, T, Hecker, M, Trepel, M, Katus, HA *et al.* (2012). Novel random peptide libraries displayed on AAV serotype 9 for selection of endothelial cell-directed gene transfer vectors. *Gene Ther* **19**: 800–809.
- Asokan, A, Hamra, JB, Govindasamy, L, Agbandje-McKenna, M and Samulski, RJ (2006). Adeno-associated virus type 2 contains an integrin  $\alpha 5\beta 1$  binding domain essential for viral cell entry. *J Virol* **80**: 8961–8969.
- Summerford, C, Bartlett, JS and Samulski, RJ (1999). AlphaVbeta5 integrin: a co-receptor for adeno-associated virus type 2 infection. *Nat Med* **5**: 78–82.
- Summerford, C and Samulski, RJ (1998). Membrane-associated heparan sulfate proteoglycan is a receptor for adeno-associated virus type 2 virions. *J Virol* **72**: 1438–1445.
- Asselineau, D, Bernhard, B, Bailly, C and Darmon, M (1985). Epidermal morphogenesis and induction of the 67 kD keratin polypeptide by culture of human keratinocytes at the liquid-air interface. *Exp Cell Res* **159**: 536–539.
- Di Pasquale, G, Davidson, BL, Stein, CS, Martins, I, Scudiero, D, Monks, A *et al.* (2003). Identification of PDGFR as a receptor for AAV-5 transduction. *Nat Med* **9**: 1306–1312.
- Kondratowicz, AS, Lennemann, NJ, Sinn, PL, Davey, RA, Hunt, CL, Moller-Tank, S *et al.* (2011). T-cell immunoglobulin and mucin domain 1 (TIM-1) is a receptor for Zaire Ebolavirus and Lake Victoria Marburgvirus. *Proc Natl Acad Sci USA* **108**: 8426–8431.
- Quinn, K, Brindley, MA, Weller, ML, Kaludov, N, Kondratowicz, A, Hunt, CL *et al.* (2009). Rho GTPases modulate entry of Ebola virus and vesicular stomatitis virus pseudotyped vectors. *J Virol* **83**: 10176–10186.
- Weller, ML, Amornphimoltham, P, Schmidt, M, Wilson, PA, Gutkind, JS and Chiorini, JA (2010). Epidermal growth factor receptor is a co-receptor for adeno-associated virus serotype 6. *Nat Med* **16**: 662–664.
- Humphries, JD, Byron, A and Humphries, MJ (2006). Integrin ligands at a glance. *J Cell Sci* **119**(Pt 19): 3901–3903.
- Jackson, T, Clark, S, Berryman, S, Burman, A, Cambier, S, Mu, D *et al.* (2004). Integrin  $\alpha 5\beta 8$  functions as a receptor for foot-and-mouth disease virus: role of the beta-chain cytodomain in integrin-mediated infection. *J Virol* **78**: 4533–4540.
- Mu, D, Cambier, S, Fjellbirkeland, L, Baron, JL, Munger, JS, Kawakatsu, H *et al.* (2002). The integrin  $\alpha (v)\beta 8$  mediates epithelial homeostasis through MT1-MMP-dependent activation of TGF- $\beta 1$ . *J Cell Biol* **157**: 493–507.
- Johns, HL, Berryman, S, Monaghan, P, Belsham, GJ and Jackson, T (2009). A dominant-negative mutant of rab5 inhibits infection of cells by foot-and-mouth disease virus: implications for virus entry. *J Virol* **83**: 6247–6256.
- Wang, LH, Rothberg, KG and Anderson, RG (1993). Mis-assembly of clathrin lattices on endosomes reveals a regulatory switch for coated pit formation. *J Cell Biol* **123**: 1107–1117.
- Van Hamme, E, Dowerchin, HL, Cornelissen, E, Verhasselt, B and Nauwynck, HJ (2008). Clathrin- and caveolae-independent entry of feline infectious peritonitis virus in monocytes depends on dynamin. *J Gen Virol* **89**(Pt 9): 2147–2156.
- Eming, SA, Krieg, T and Davidson, JM (2007). Inflammation in wound repair: molecular and cellular mechanisms. *J Invest Dermatol* **127**: 514–525.
- Schechner, JS, Crane, SK, Wang, F, Szeplin, AM, Tlides, G, Lorber, MI *et al.* (2003). Engraftment of a vascularized human skin equivalent. *FASEB J* **17**: 2250–2256.
- De Luca, M, Pellegrini, G and Mavilio, F (2009). Gene therapy of inherited skin adhesion disorders: a critical overview. *Br J Dermatol* **161**: 19–24.
- Zhong, L, Li, B, Jayandharan, G, Mah, CS, Govindasamy, L, Agbandje-McKenna, M *et al.* (2008). Tyrosine-phosphorylation of AAV2 vectors and its consequences on viral intracellular trafficking and transgene expression. *Virology* **381**: 194–202.
- Zhong, L, Li, B, Mah, CS, Govindasamy, L, Agbandje-McKenna, M, Cooper, M *et al.* (2008). Next generation of adeno-associated virus 2 vectors: point mutations in

- tyrosines lead to high-efficiency transduction at lower doses. *Proc Natl Acad Sci USA* **105**: 7827–7832.
41. Grimm, D, Lee, JS, Wang, L, Desai, T, Akache, B, Storm, TA *et al.* (2008). *In vitro* and *in vivo* gene therapy vector evolution via multispecies interbreeding and retargeting of adeno-associated viruses. *J Virol* **82**: 5887–5911.
  42. Michelfelder, S, Kohlschütter, J, Skorupa, A, Pfennings, S, Müller, O, Kleinschmidt, JA *et al.* (2009). Successful expansion but not complete restriction of tropism of adeno-associated virus by *in vivo* biopanning of random virus display peptide libraries. *PLoS ONE* **4**: e5122.
  43. Naumer, M, Ying, Y, Michelfelder, S, Reuter, A, Trepel, M, Müller, OJ *et al.* (2012). Development and validation of novel AAV2 random libraries displaying peptides of diverse lengths and at diverse capsid positions. *Hum Gene Ther* **23**: 492–507.
  44. Ying, Y, Müller, OJ, Goehring, C, Leuchs, B, Trepel, M, Katus, HA *et al.* (2010). Heart-targeted adeno-associated viral vectors selected by *in vivo* biopanning of a random viral display peptide library. *Gene Ther* **17**: 980–990.
  45. Uhrig, S, Coutelle, O, Wiehe, T, Perabo, L, Hallek, M and Büning, H (2012). Successful target cell transduction of capsid-engineered rAAV vectors requires clathrin-dependent endocytosis. *Gene Ther* **19**: 210–218.
  46. Cambier, S, Mu, DZ, O'Connell, D, Boylen, K, Travis, W, Liu, WH *et al.* (2000). A role for the integrin  $\alpha$ v $\beta$ 8 in the negative regulation of epithelial cell growth. *Cancer Res* **60**: 7084–7093.
  47. Stachelscheid, H, Ibrahim, H, Koch, L, Schmitz, A, Tschardt, M, Wunderlich, FT *et al.* (2008). Epidermal insulin/IGF-1 signalling control interfollicular morphogenesis and proliferative potential through Rac activation. *EMBO J* **27**: 2091–2101.
  48. Girod, A, Ried, M, Wobus, C, Lahm, H, Leike, K, Kleinschmidt, J *et al.* (1999). Genetic capsid modifications allow efficient re-targeting of adeno-associated virus type 2. *Nat Med* **5**: 1052–1056.
  49. Hacker, UT, Wingenfeld, L, Kofler, DM, Schuhmann, NK, Lutz, S, Herold, T *et al.* (2005). Adeno-associated virus serotypes 1 to 5 mediated tumor cell directed gene transfer and improvement of transduction efficiency. *J Gene Med* **7**: 1429–1438.
  50. Xiao, X, Li, J and Samulski, RJ (1998). Production of high-titer recombinant adeno-associated virus vectors in the absence of helper adenovirus. *J Virol* **72**: 2224–2232.